

COHESIVE CRACK PROPAGATION IN DAMAGING CONCRETE STRUCTURES DISCRETIZED BY EXTENDED FINITE ELEMENTS

C. COMI¹, S. MARIANI², U. PEREGO³

Dipartimento di Ingegneria Strutturale, Politecnico di Milano, Milano (ITALY)

¹claudia.comi@polimi.it, ²stefano.mariani@polimi.it, ³umberto.perego@polimi.it

ABSTRACT

A coupled continuum damage-discrete crack propagation strategy to simulate strength degradation and fracture in concrete structures is presented. At fixed crack length, mesh-independent results are obtained through an integral non-local regularization of the damage model. For increasing loading conditions, as soon as a critical damage threshold is attained in the process zone, cohesive cracks are introduced to allow for a discontinuous displacement field. Within the class of cohesive laws that feature the same dissipation properties of the continuum damage model, constitutive parameters are calibrated through an energy equivalence. Results concerning the wedge splitting test are shown to demonstrate the efficiency of the proposed procedure.

1 INTRODUCTION

The response of concrete structures to increasing loadings is characterized in the early stage by the spreading of micro-cracks in localized regions (like, e.g., ahead of a pre-existing notch); these micro-cracks eventually coalesce to create only a few macro-cracks.

To simulate numerically this complex behavior, a continuum damage approach proves efficient in the first stage. But, for increasing levels of damage, the width of the band where damage still continues to grow tends to become narrower and narrower. To accurately resolve the process zone, the characteristic dimension of finite elements needs to be a fraction of the bandwidth. If it is chosen small enough from the beginning of the analysis, computational costs become excessive for real-life structures like, e.g., concrete dams. Otherwise, the mesh can be adaptively refined during the analysis so as to simulate the process zone response with the required degree of accuracy; in this case the computational burden is mainly due to the continuous projection of current results from the old meshes to the new ones.

In this work an alternative approach is followed. From a simplified bifurcation analysis of a one-dimensional elastic damage continuum subject to a uniform stress and strain distribution, an estimate of the process zone width as a function of damage is obtained [1]. At fixed discretization, as soon as the mesh is considered too coarse to resolve the band on the basis of the above estimate, a cohesive crack is allowed for through the partition of unity concept [2, 3, 4]. As shown in [4], under mixed mode loading conditions this methodology allows to simulate crack paths completely independent of the mesh layout.

Concerning the constitutive modeling of concrete, an integral non-local regularization is adopted to restore the well-posedness of the set of equations governing the problem [5, 6]. This allows to fix the fracture energy, that is the energy to be dissipated in order to completely annihilate the interaction between the two faces of the crack. The cohesive model can thus be calibrated by allowing the crack to dissipate only the fraction of the concrete toughness not already dissipated by the continuum prior to crack insertion.

This procedure is numerically tested with an analysis of the failure mechanism in the wedge splitting test [7], where a pre-existing edge notch is subject to mode I loading. It is shown that, when the displacement discontinuity is plugged into the simulation, a realistic damage pattern around the propagating macro-crack is obtained.

2 GOVERNING RELATIONS

Let us consider a two-dimensional (2D) solid Ω , with boundary $\Gamma = \Gamma_u \cup \Gamma_t$ (Fig. 1). Traction $\bar{\mathbf{t}}$ are prescribed on Γ_t , whereas displacements $\bar{\mathbf{u}}$ are assigned on Γ_u . A displacement discontinuity locus Γ_d can

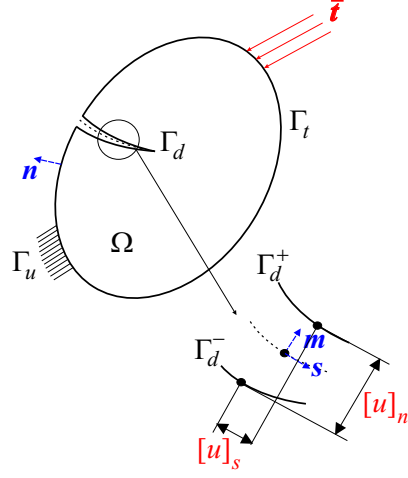


Figure 1: 2D solid. Geometry and notation.

nucleate and propagate inside Ω .

Under the assumption of linearized kinematics, equilibrium and compatibility relations for Ω are:

$$\begin{aligned}
 \mathcal{C}^T \boldsymbol{\sigma} + \bar{\mathbf{b}} &= \mathbf{0} && \text{in } \Omega \setminus \Gamma_d && (1) \\
 \mathbf{N} \boldsymbol{\sigma} &= \bar{\mathbf{t}} && \text{on } \Gamma_t && (2) \\
 \mathbf{M} \boldsymbol{\sigma} = -\mathbf{t}^+ & \text{ on } \Gamma_d^+, & \mathbf{M} \boldsymbol{\sigma} = \mathbf{t}^- & \text{ on } \Gamma_d^-, & \mathbf{t} \equiv \mathbf{t}^- = -\mathbf{t}^+ && (3) \\
 \boldsymbol{\varepsilon} &= \mathcal{C} \mathbf{u} && \text{in } \Omega \setminus \Gamma_d && (4) \\
 \mathbf{u} &= \bar{\mathbf{u}} && \text{on } \Gamma_u && (5) \\
 [\mathbf{u}] &= \mathbf{u}|_{\Gamma_d^+} - \mathbf{u}|_{\Gamma_d^-} && && (6)
 \end{aligned}$$

where: \mathbf{u} is the displacement vector; $[\mathbf{u}]$ is the displacement discontinuity vector along Γ_d ; $\boldsymbol{\varepsilon}$ and $\boldsymbol{\sigma}$ are the strain and stress vectors; $\bar{\mathbf{t}}$ are the tractions acting upon the boundary of Ω (Γ_d included); \mathcal{C} is the differential compatibility operator; \mathbf{N} and \mathbf{M} are matrices gathering the components of unit vectors \mathbf{n} and \mathbf{m} (see Fig. 1); T stands for transpose; Γ_d^+ and Γ_d^- denote the two sides of Γ_d , according to Fig. 1.

An isotropic elastic damage constitutive law is adopted for $\Omega \setminus \Gamma_d$. The local format of this law reads:

$$\boldsymbol{\sigma} = (1 - D) \mathbf{E} : \boldsymbol{\varepsilon} \quad (7)$$

$$f = 2\mu^2 \mathbf{e} : \mathbf{e} - 9K^2 a \varepsilon_v^2 + 3Kb \ln^{\frac{n}{2}} \left(\frac{c}{1-D} \right) \varepsilon_v - k \ln^n \left(\frac{c}{1-D} \right) \leq 0 \quad (8)$$

$$\dot{D} \geq 0, \quad f \dot{D} = 0 \quad (9)$$

where: \mathbf{E} is the matrix of elastic moduli of the virgin material; D is the isotropic damage variable; μ and K are the shear and bulk elastic moduli; f is the damage activation function; ε_v is the volumetric strain, whereas \mathbf{e} is the deviator of $\boldsymbol{\varepsilon}$; a, b, c, k and n are model parameters, to be adjusted in order to match the

concrete behavior in the softening regime. The continuum model (7)-(9) locally dissipates a specific energy:

$$g_f = \frac{1}{2} \frac{\sigma_0^2}{E} \left\{ 1 + \frac{2^n c}{n^{n-1}} G[n, \ln c] \right\} \quad (10)$$

Here: E is the Young's modulus of the virgin material; σ_0 is the peak strength under uniaxial tensile loadings; $G[n, \ln c] \equiv \int_{\ln c}^{\infty} z^{n-1} \exp(-z) dz$ is the incomplete gamma function.

To restore the well-posedness of the problem (1)-(9) in the softening regime (when $\dot{D} > 0$) and to achieve mesh-independent results an integral non-local regularization of the strain invariants is adopted [5, 6].

As for Γ_d , the cohesive law $\mathbf{t} = \mathbf{t}([u])$ is formulated so as to feature a softening envelope similar to that of the damage model for the bulk [8]. Model parameters are calibrated in order to get the same energy dissipation in the following two cases: (a) a continuum analysis allowing for bulk damage only, without crack growth; (b) an enhanced analysis with bulk damage coupled to crack propagation as soon as a critical damage threshold is attained in the process zone (for details see [8]). It turns out that, under mode I loadings:

$$t_n([u]_n) = c \exp \left[- \left(\frac{b + \sqrt{b^2 + 4 \left(\frac{1}{3} - a \right) k}}{2k} E \left(\varepsilon_c + \frac{[u]_n}{L_e} \right) \right)^{\frac{2}{n}} \right] E \left(\varepsilon_c + \frac{[u]_n}{L_e} \right) + \frac{1}{2} E (1 - D_c) \varepsilon_c^2 \frac{[u]_n}{L_e} \exp \left[- \frac{[u]_n}{L_e} \right] \quad (11)$$

where: t_n and $[u]_n$ are, respectively, the opening traction and displacement discontinuity (see Fig. 1); D_c is the mentioned critical damage threshold and ε_c the relevant deformation in Ω ; L_e is the width of the process zone corresponding to D_c [1].

3 FINITE ELEMENT FORMULATION

Within the frame of the extended finite element method, the assumed discretized displacement field is:

$$\mathbf{u}^h(\mathbf{x}) = \sum_{i \in I} \phi_i(\mathbf{x}) \mathbf{u}_i^0 + \sum_{j \in J} \mathcal{H}(\mathbf{x}) \phi_j(\mathbf{x}) \mathbf{u}_j^E \quad (12)$$

where: \mathbf{x} is the position vector in the 2D space; the node set I covers the whole domain Ω , while the set J gathers only those nodes whose support ω_j is even partially cut by Γ_d ; ϕ_i is the piecewise linear nodal shape function; \mathbf{u}_i^0 are the basic degrees of freedom (DOFs) and \mathbf{u}_j^E are the additional, or extended ones; $\mathcal{H}(\mathbf{x})$ is the generalized Heaviside step-function, defined according to:

$$\mathcal{H}(\mathbf{x}) = \begin{cases} +1 & \text{if } (\mathbf{x} - \mathbf{x}^*)^T \mathbf{m} > 0 \\ -1 & \text{if } (\mathbf{x} - \mathbf{x}^*)^T \mathbf{m} < 0 \end{cases} \quad (13)$$

\mathbf{x}^* being the closest point projection of \mathbf{x} onto Γ_d .

To avoid locking of the discrete formulation when a collapse mechanism is developed in the structure after complete crack growth, all the nodes belonging to the tip element are included in the set J .

Now, let e_1, e_2, e_3 be the vertex nodes of a generic triangular element e , whose domain is Ω_e . If all the three

nodes belong to set J , the in-plane displacement field $\mathbf{u}^h(\mathbf{x})$ reads:

$$\mathbf{u}^h(\mathbf{x}) = \begin{Bmatrix} u_x^h(\mathbf{x}) \\ u_y^h(\mathbf{x}) \end{Bmatrix} = [\Phi_e \quad \vdots \quad \mathcal{H}\Phi_e] \begin{Bmatrix} \mathbf{u}_e^0 \\ \vdots \\ \mathbf{u}_e^E \end{Bmatrix} \quad \mathbf{x} \in \Omega_e \quad (14)$$

where \mathbf{u}_e^0 and \mathbf{u}_e^E respectively gather all the basic and extended nodal DOFs relevant to element e and Φ_e is the standard matrix of interpolation functions, i.e.:

$$\Phi_e = \begin{bmatrix} \phi_{e1} & 0 & \phi_{e2} & 0 & \phi_{e3} & 0 \\ 0 & \phi_{e1} & 0 & \phi_{e2} & 0 & \phi_{e3} \end{bmatrix} \quad (15)$$

The strain field is thus given by:

$$\boldsymbol{\varepsilon}^h(\mathbf{x}) = \begin{Bmatrix} \varepsilon_x^h(\mathbf{x}) \\ \varepsilon_y^h(\mathbf{x}) \\ 2\varepsilon_{xy}^h(\mathbf{x}) \end{Bmatrix} = [\mathbf{B}_e \quad \vdots \quad \mathcal{H}\mathbf{B}_e] \begin{Bmatrix} \mathbf{u}_e^0 \\ \vdots \\ \mathbf{u}_e^E \end{Bmatrix} \quad \mathbf{x} \in \Omega_e \setminus \Gamma_{de} \quad (16)$$

Γ_{de} being the portion of Γ_d inside element e and:

$$\mathbf{B}_e = \begin{bmatrix} \phi_{e1,x} & 0 & \phi_{e2,x} & 0 & \phi_{e3,x} & 0 \\ 0 & \phi_{e1,y} & 0 & \phi_{e2,y} & 0 & \phi_{e3,y} \\ \phi_{e1,y} & \phi_{e1,x} & \phi_{e2,y} & \phi_{e2,x} & \phi_{e3,y} & \phi_{e3,x} \end{bmatrix} \quad (17)$$

Here a comma means derivative.

The discretized displacement discontinuity along Γ_{de} is:

$$[\mathbf{u}]^h(\mathbf{x}) = \mathbf{u}^h \Big|_{\Gamma_{de}^+} - \mathbf{u}^h \Big|_{\Gamma_{de}^-} = \sum_{j \in J} 2\phi_j(\mathbf{x}) \mathbf{u}_j^E = [\mathbf{0} \quad \vdots \quad 2\Phi_e] \begin{Bmatrix} \mathbf{u}_e^0 \\ \vdots \\ \mathbf{u}_e^E \end{Bmatrix} \quad \mathbf{x} \in \Gamma_{de} \quad (18)$$

During the analysis, at fixed crack length the damage D^h at Gauss points is continuously monitored; in all the elements where D^h exceeds the critical threshold, a crack segment should be introduced. However, according to the physics of the problem explained in the introduction, only one crack is allowed to propagate inside each damage band.

To propagate Γ_d , the damage pattern in the process zone is recovered and best-fitted with a complete fourth-order polynomial. Crack growth is then chosen to be perpendicular to the direction of maximum curvature of the interpolating polynomial at the crack tip.

4 NUMERICAL SIMULATION OF THE WEDGE-SPLITTING TEST

The wedge splitting test configuration is shown in Fig. 2 (specimen thickness is 97 mm). Experimentally, a wedge is pushed from the left into the side notch so that two opposite forces (P) act at the mouth of the initial crack and cause a mode I propagation. The ligament, where the process zone develops, is thus subject to bending.

To simulate damage evolution in the bulk, the following values of model parameters have been adopted: $E = 25200$ MPa; $\nu = 0.2$; $a = 0.2$; $b = 0.1265$ MPa; $c = 10000$; $k = 6.838 \cdot 10^{-7}$ MPa²; $n = 12$. The internal length scale for the non-local regularization has been assumed $l_c = 17.5$ mm. These material

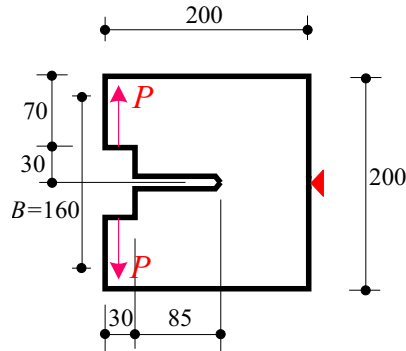


Figure 2: Wedge splitting test. Geometry and loading conditions.

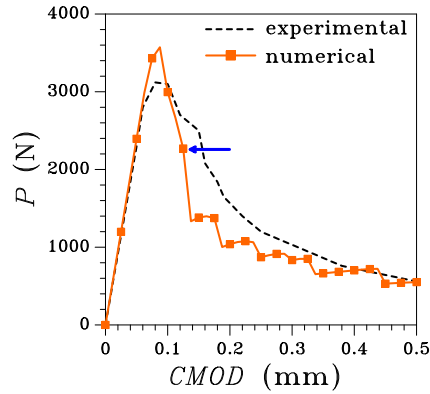


Figure 3: Wedge splitting test. Load vs $CMOD$ response.

parameters correspond to a concrete tensile strength $\sigma^M = 3.3$ MPa and to a mode I fracture toughness $G_f \approx 100$ J/m².

In the analysis, crack propagation is simulated under $CMOD$ (crack mouth opening displacement) control. The numerical P vs $CMOD$ response is compared in Fig. 3 to the available experimental data [7]. In view of the rather rough calibration of the model, the softening branch can be considered to reproduce the actual response with an encouraging level of accuracy. The blue arrow in the figure points towards the onset of crack growth: the initial post peak strength reduction is thus caused by bulk damage only.

In Fig. 4 level sets of damage D are reported in the deformed configuration, with displacements amplified 100 times to appraise crack growth. It can be seen that, after an initial transient phase, damage evolves maintaining an almost constant bandwidth in the process zone ahead of the current crack tip.

ACKNOWLEDGMENTS

This work has been carried out with the financial support of MIUR-PRIN 2002087915-2002 contract.

REFERENCES

- [1] C. Comi and U. Perego. Criteria for mesh refinement in nonlocal damage finite element analyses. *European Journal of Mechanics A/Solids*, in press, 2004.

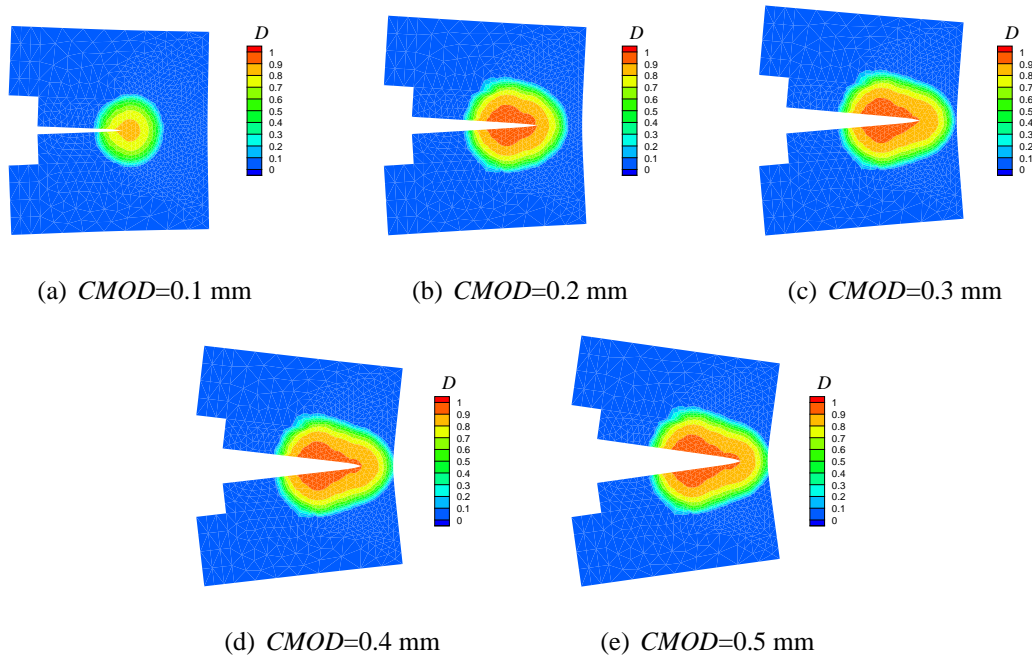


Figure 4: Wedge splitting test. Simulated damage evolution and crack growth.

- [2] N. Moës, J. Dolbow, and T. Belytschko. A finite element method for crack growth without remeshing. *International Journal for Numerical Methods in Engineering*, 46:131–150, 1999.
- [3] G.N. Wells and L.J. Sluys. A new method for modelling cohesive cracks using finite elements. *International Journal for Numerical Methods in Engineering*, 50:2667–2682, 2001.
- [4] S. Mariani and U. Perego. Extended finite element method for quasi-brittle fracture. *International Journal for Numerical Methods in Engineering*, 58:103–126, 2003.
- [5] M. Jirasek. Nonlocal models for damage and fracture: Comparison of approaches. *International Journal of Solids and Structures*, 35:4133–4145, 1998.
- [6] C. Comi. A non-local model with tension and compression damage mechanisms. *European Journal of Mechanics A/Solids*, 20:1–22, 2001.
- [7] E. Denarié, V.E. Saouma, A. Iocco, and D. Varelas. Concrete fracture process zone characterization with fiber optics. *ASCE Journal of Engineering Mechanics*, 127:494–502, 2001.
- [8] C. Comi, S. Mariani, and U. Perego. From localized damage to discrete cohesive crack propagation in nonlocal continua. In H.A. Mang, F.G. Rammerstorfer, and J. Eberhardsteiner, editors, *Proceedings of the Fifth World Congress on Computational Mechanics (WCCM V)*. Vienna University of Technology, 2002.